The Properties of Superconducting UTe_2

Summary for students in Phys798C Superconductivity
Fall 2025 semester

Quantum Materials Center

Anlage High Frequency Superconductivity Group

University of Maryland Department of Physics

Superconducting Transition Temperatures vs. Time

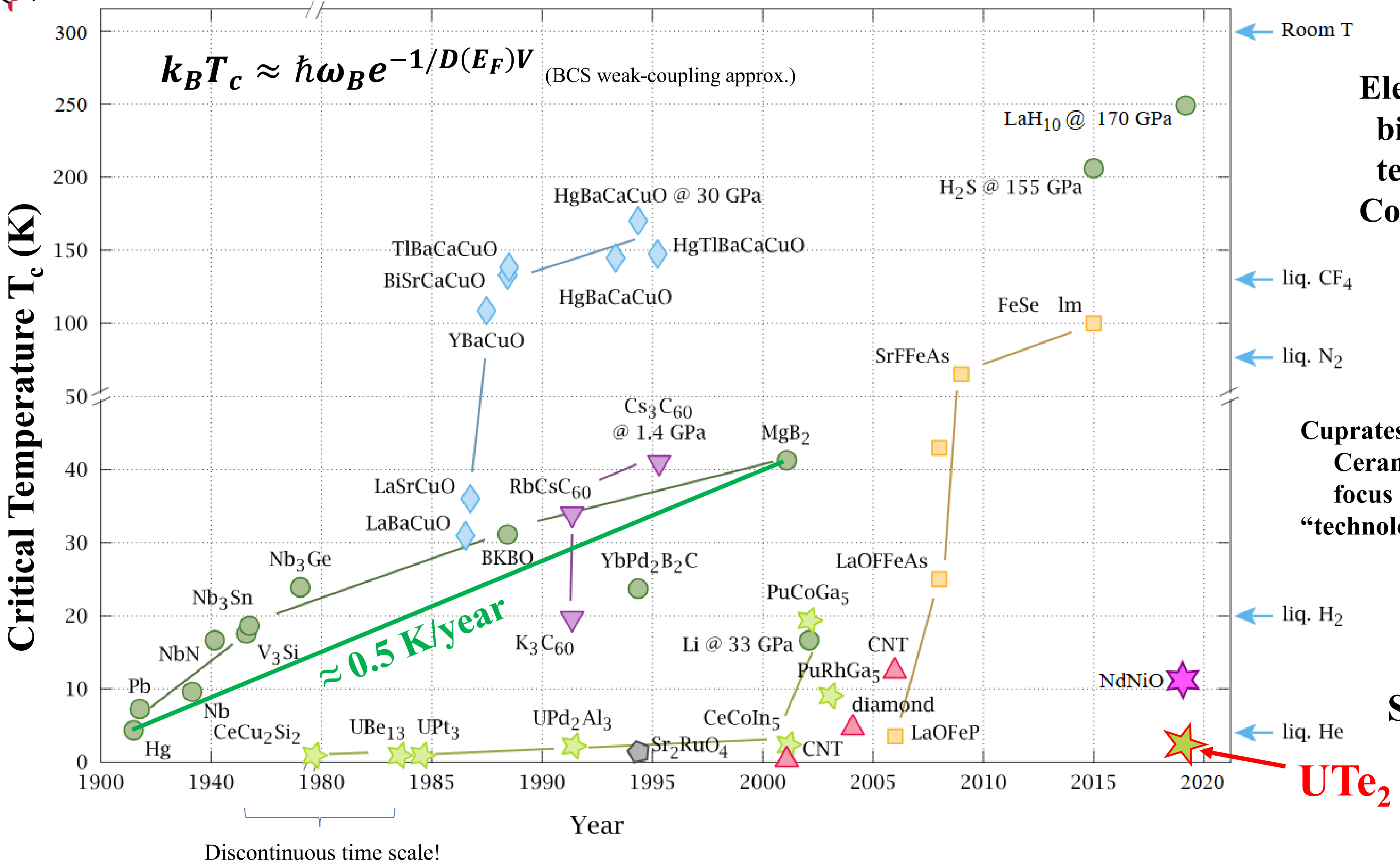

Elemental metals

binary } **compounds**
tertiary

Complex materials

Cuprates
Ceramics
focus on thin films for applications
"technologically-relevant" materials

Single crystals

https://en.wikipedia.org/wiki/Superconductivity

Superconductivity and Superfluidity

Nodal energy gap

Fermi surface

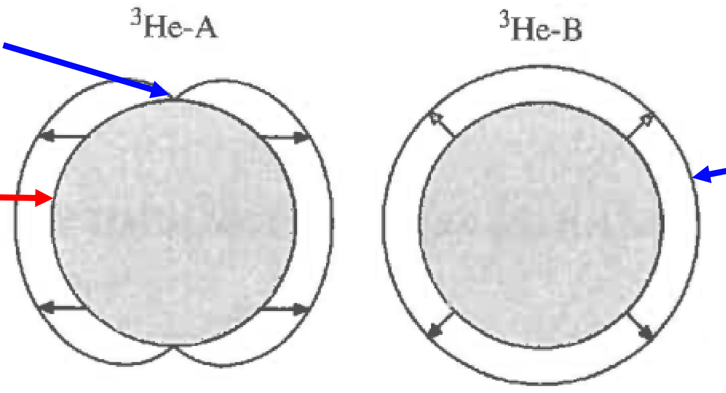

Node-less energy gap

The presence of nodes changes the low-energy excitations out of the ground state

Energy gap: $|\vec{d}(\vec{k})| \sim \sin\theta_{\vec{k}}$ $|\vec{d}(\vec{k})| \sim constant$

Are there superconducting analogs of superfluid ^{3}He?

One possibility: heavy Fermion metals

Intermetallic compounds containing Lanthanide (e.g. Ce, Yb) or Actinide (e.g. U, Np) elements with very large electron effective mass $m^{*} \sim 50 - 1000\ m_e$ at low temperatures (measured e.g. electronic specific heat)

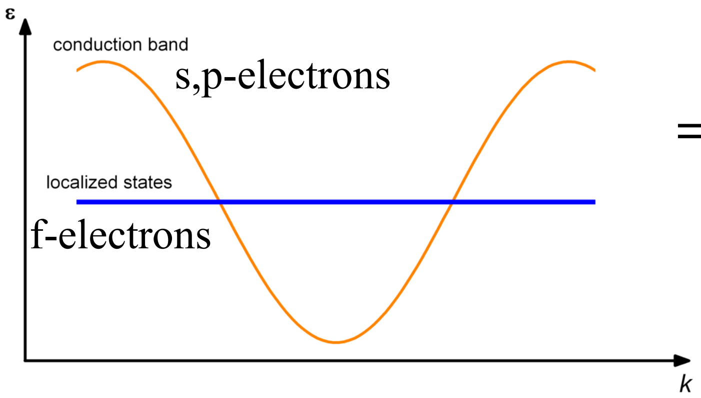

⟹ **hybridize** ⟹

Kondo physics

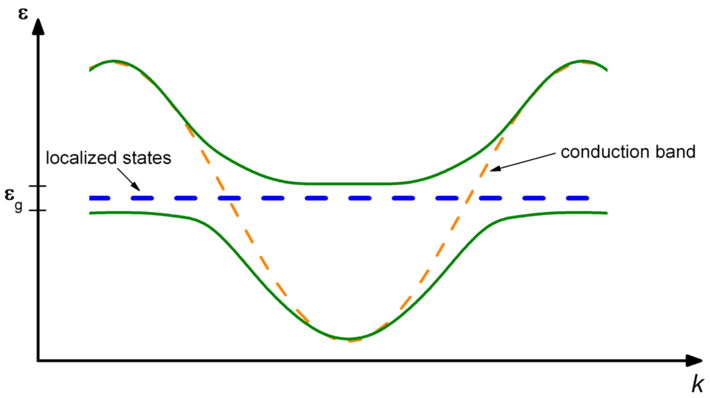

Brief overview of UTe_2 physical properties

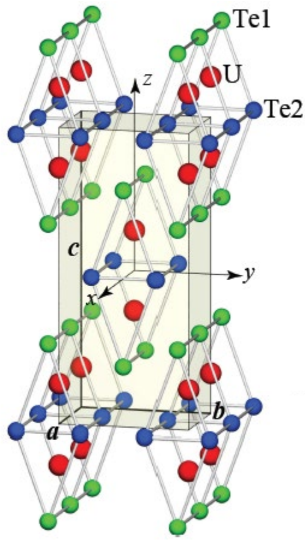

UTe_2

T_c = 1.6 K
Ran, *et al*. Science (2019)

D_{2h} point group
orthorhombic

S. Fujimori *et al*., JPSJ 88, 103701 (2019)

First generation samples showed $T_c \approx 1.6\ K$ "low-T_c" samples

Chemical vapor transport (CVT) growth

More recent generation samples show $T_c \approx 2.1\ K$ "high-T_c" samples

Molten Salt Flux (MSF) and CVT growth

Very large upper critical fields H_{c2}

$H_{c2} \gg H_{Pauli}$

$$\mu_0 H_{Pauli} = \frac{\Delta_0}{\sqrt{2}\mu_B} \approx 1.86\, T_c\ [T]$$

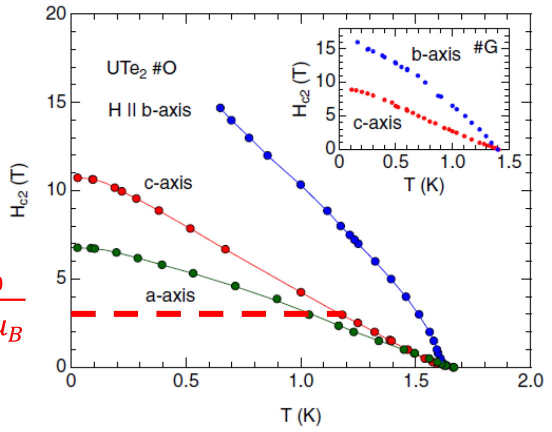

D. Aoki, *et al*., J. Phys. Soc. Jpn. 88, 043702 (2019)

Small drop in Knight shift below T_c G. Nakamine, *et al*., J. Phys. Soc. Jpn. 88, 113703 (2019)

Re-entrant superconductivity in a field-polarized phase

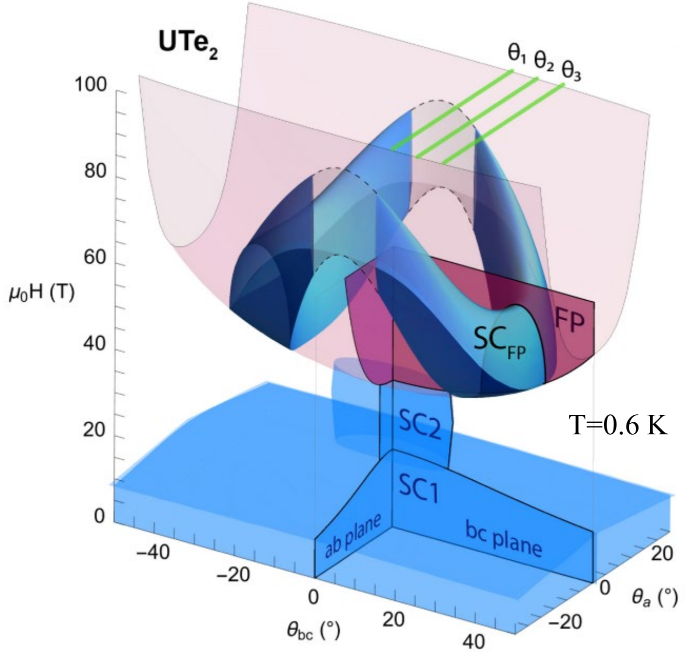

S. Ran, *et al.* Nature Physics 15, 1250 (2019)
S. K. Lewin, *et al*., Rep. Prog. Phys. 86, 114501 (2023)
S. K. Lewin, *et al*., Science 389, 512 (2025)

It is widely agreed that UTe_2 shows spin-triplet pairing

Brief overview of UTe_2 physical properties

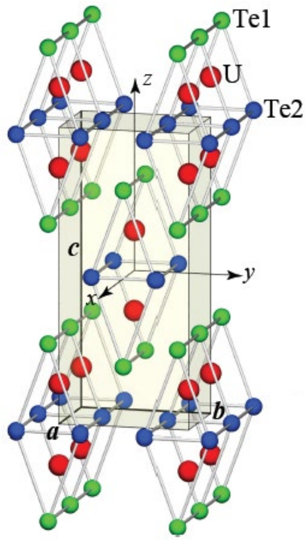

UTe_2

T_c = 1.6 K
Ran, *et al*. Science (2019)

D_{2h} point group
orthorhombic

S. Fujimori *et al*., JPSJ 88, 103701 (2019)

First generation samples showed $T_c \approx 1.6\ K$ "low-T_c" samples

Chemical vapor transport (CVT) growth

More recent generation samples show $T_c \approx 2.1\ K$ "high-T_c" samples

Molten Salt Flux (MSF) and CVT growth

Very large upper critical fields H_{c2}

$H_{c2} \gg H_{Pauli}$

$\mu_0 H_{Pauli} = \frac{\Delta_0}{\sqrt{2}\mu_B} \approx 1.86\, T_c\ [T]$

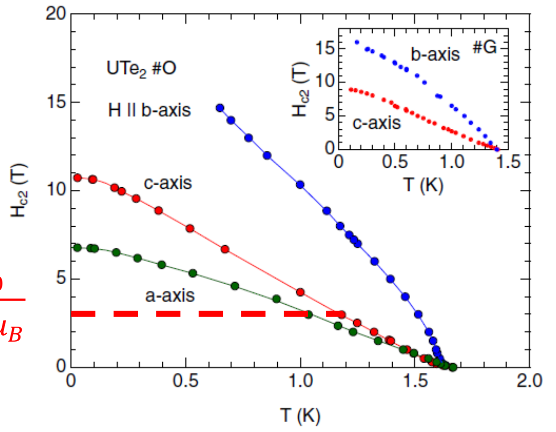

D. Aoki, *et al*., J. Phys. Soc. Jpn. 88, 043702 (2019)

Re-entrant superconductivity in a field-polarized phase

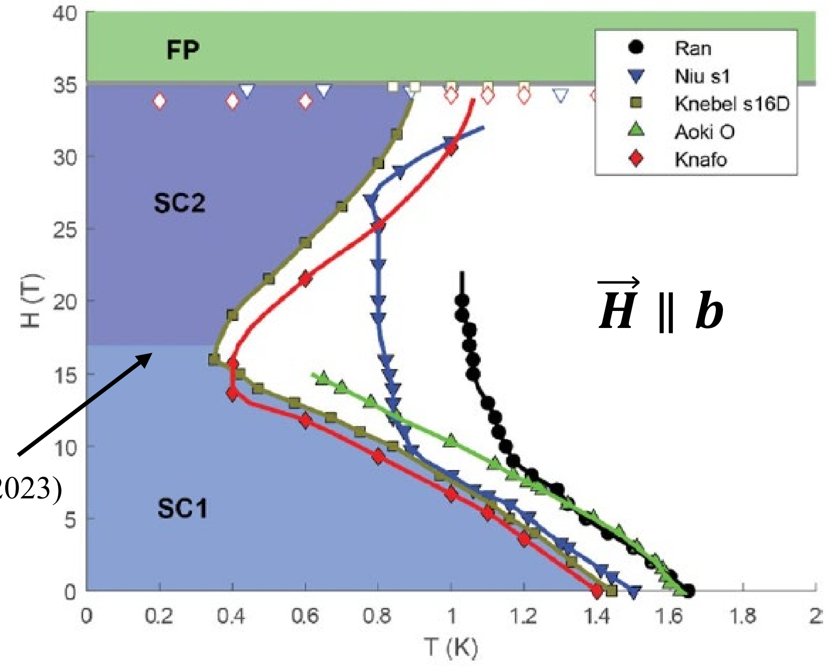

Peak in C/T seen
A. Rosuel, PRX (2023)

It is widely agreed that UTe_2 shows spin-triplet pairing

Small drop in Knight shift below T_c G. Nakamine, *et al*., J. Phys. Soc. Jpn. 88, 113703 (2019)

S. Ran, *et al.* Nature Physics 15, 1250 (2019)
S. K. Lewin, *et al*., Rep. Prog. Phys. 86, 114501 (2023)
S. K. Lewin, *et al*., Science 389, 512 (2025)

Consequences of spin-triplet Pairing in UTe_2

Oversimplified (but useful) argument:

$$\Psi_{2-electron}(\vec{r}_1, \vec{r}_2) \propto \psi(\vec{r})\,|spin-1\rangle$$

Cooper pair

Exchange: **odd** **odd** **even**

$\ell = 1$, ***p-wave* superconductor**

R. Balian and N. R. Werthamer, "Superconductivity with Pairs in a Relative p Wave," Phys Rev **131 (4), 1553–1564 (1963).**

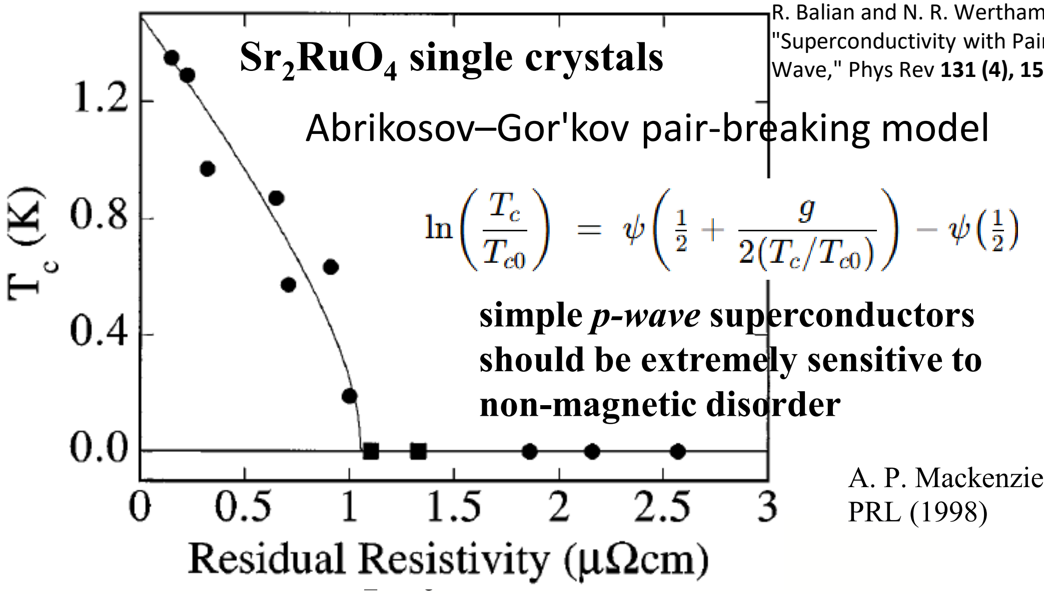

A. P. Mackenzie, *et al.* PRL (1998)

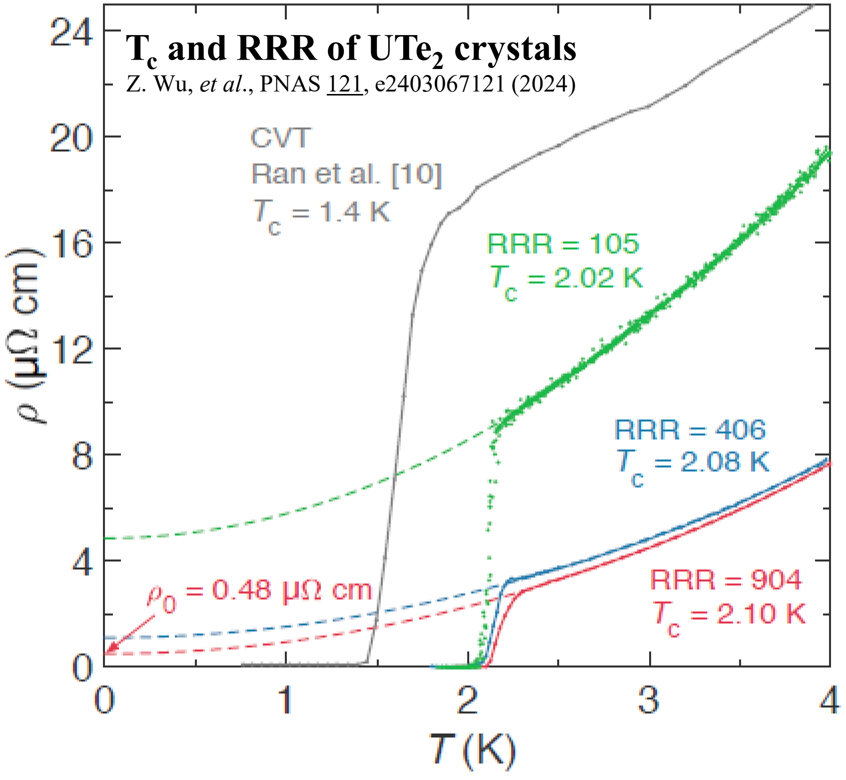

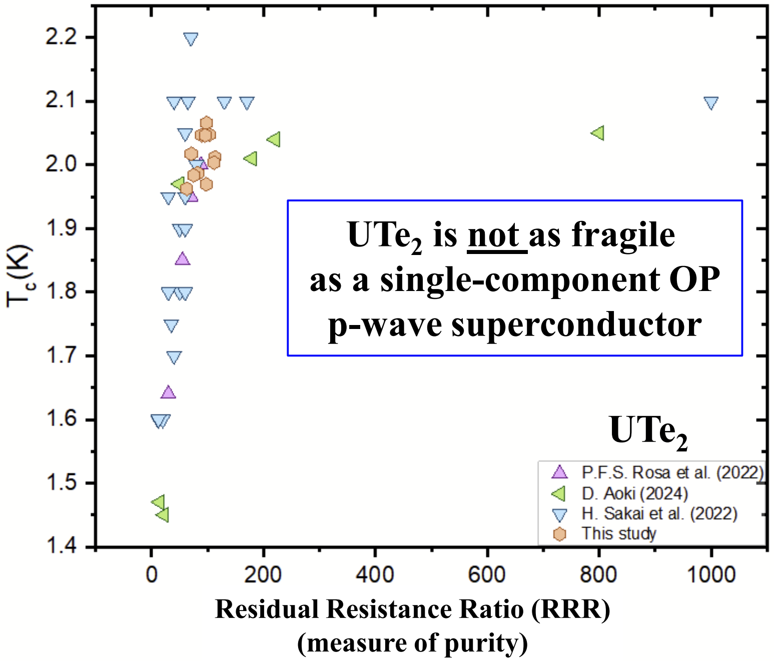

Gicela Saucedo, UMD

Evidence for Multi-Component Order Parameter in UPt_3

VOLUME 62, NUMBER 12 PHYSICAL REVIEW LETTERS 20 MARCH 1989

Specific Heat of UPt_3: Evidence for Unconventional Superconductivity

R. A. Fisher, S. Kim, B. F. Woodfield, and N. E. Phillips

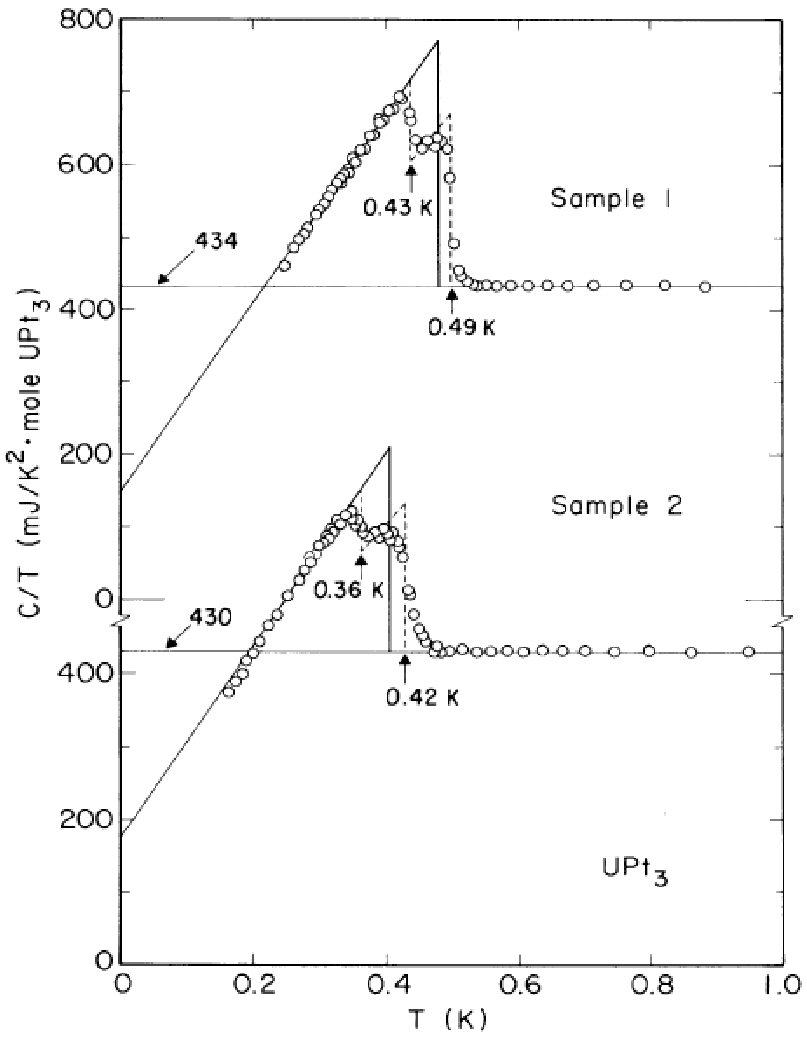

VOLUME 65, NUMBER 18 PHYSICAL REVIEW LETTERS 29 OCTOBER 1990

Phase Diagram of UPt_3 from Ultrasonic Velocity Measurements

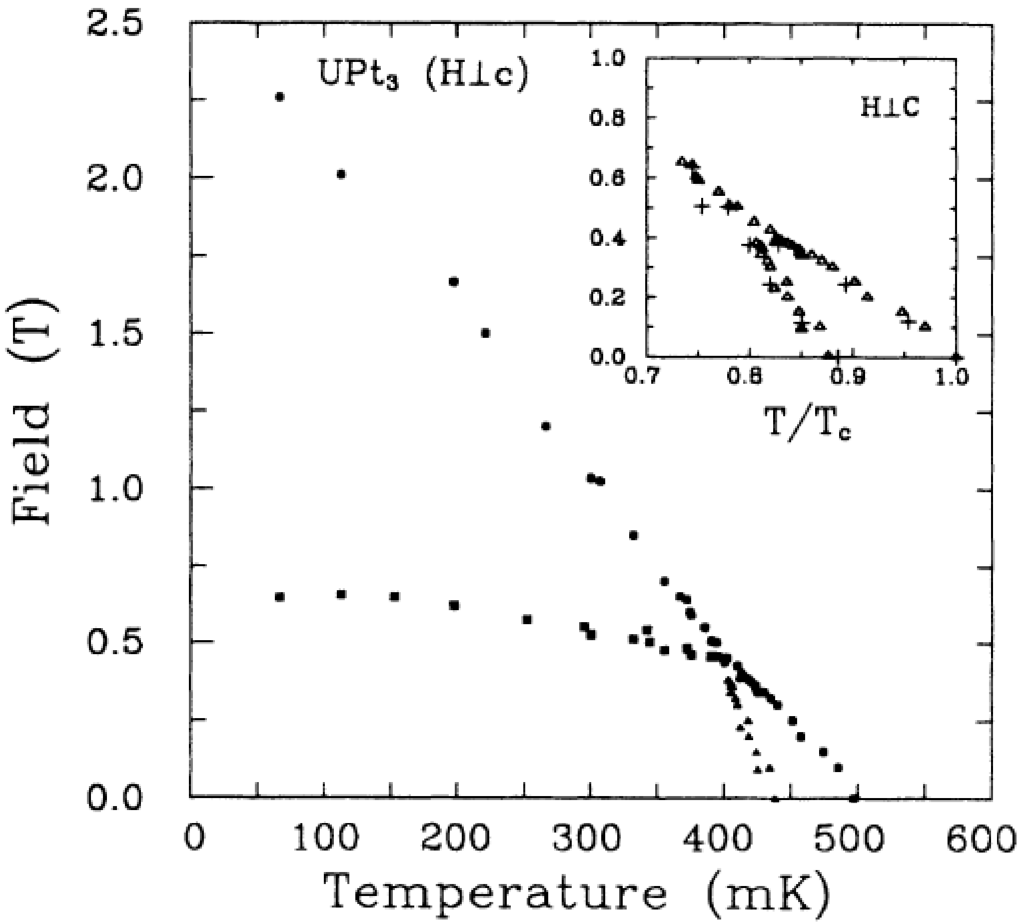

Evidence of Multi-Component Order Parameter in UTe_2

For example $p_x + ip_y$, with broken time-reversal invariance

Multicomponent superconducting order parameter in UTe_2 Science 373, 797–801 (2021)

I. M. Hayes[1]†, D. S. Wei[2,3]†, T. Metz[1], J. Zhang[4], Y. S. Eo[1], S. Ran[1,5], S. R. Saha[1,5], J. Collini[1], N. P. Butch[1,5], D. F. Agterberg[6], A. Kapitulnik[2,3,7,8]*, J. Paglione[1,5,9]*

Spontaneous vortex/anti-vortex pairs in zero field

scanning SQUID microscope images of UTe_2

Iguchi, *et al.*, PRL 130, 196003 (2023)

Two transitions in specific heat

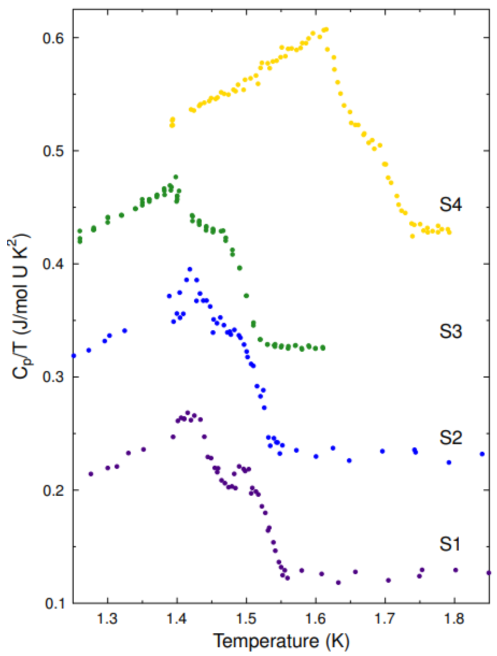

Non-zero polar Kerr effect below T_c

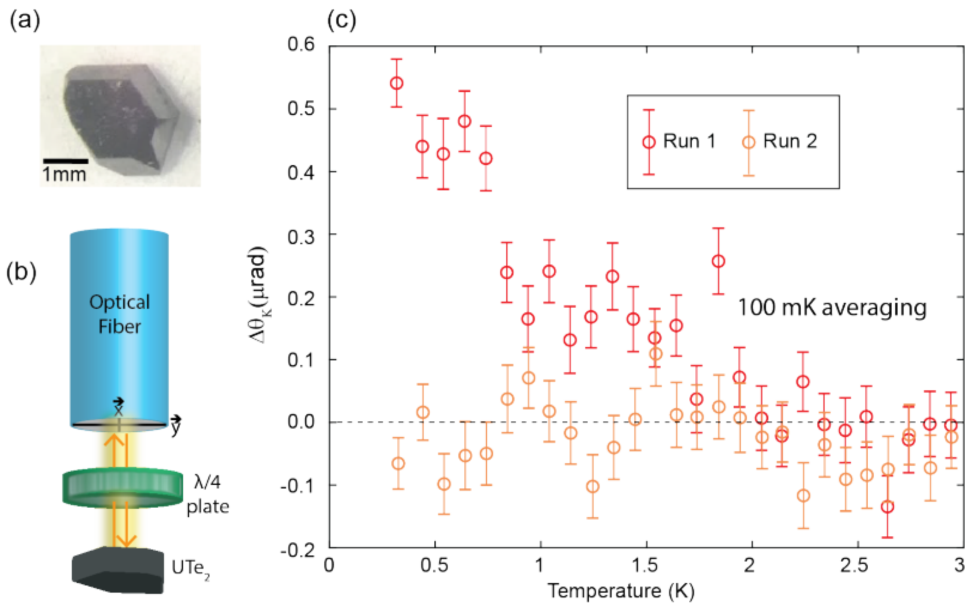

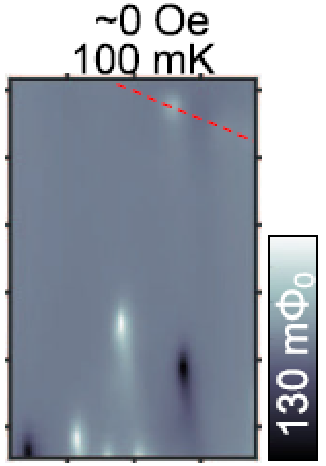

… and other results …

► **UTe_2 *may* be characterized by a two-component order parameter that breaks time-reversal symmetry …**

Evidence of Single-Component Order Parameter in UTe_2

Zero-field μSR shows no TR-breaking (Azari, PRL, 2023)

Absence of Polar Kerr in MSF-grown crystals (Ajeesh, PRX, 2023)

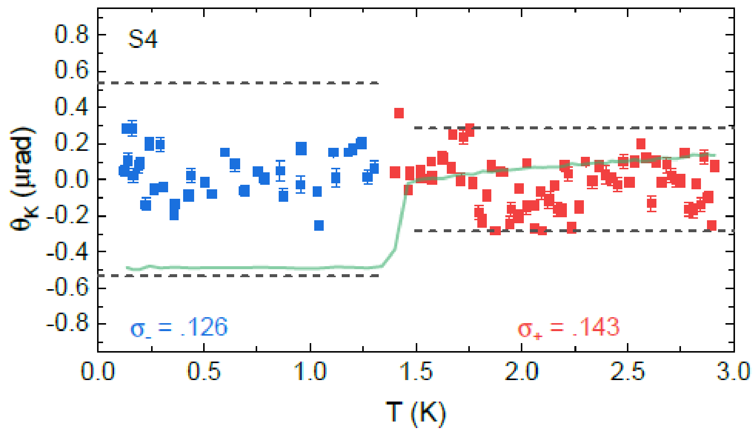

Absence of thermodynamic discontinuities in the shear elastic moduli of UTe_2 (Theuss, *et al.*, Nat. Phys. 20, 1124 (2024))

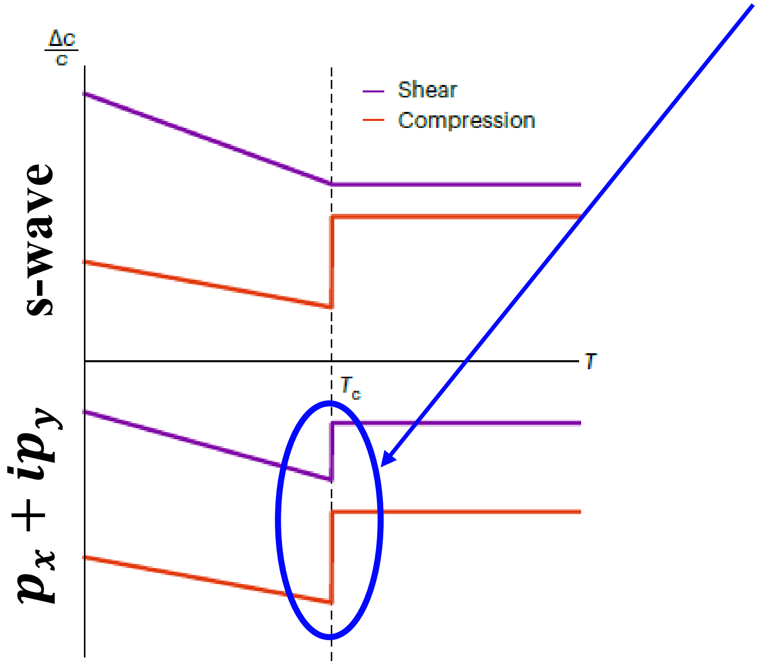

Current consensus:

Newer generation UTe_2 crystals (CVT and MSF) show no conclusive evidence of TRI-breaking in the superconducting state

“State of the Art” for the Physical Properties of UTe_2

Fall, 2025

<u>Assume</u> that there is a single-component superconducting order parameter

Order Parameter Symmetry (D_{2h} crystal point group)	Gap Nodes	Supporting Evidence (not a complete list!)
A_u	None (fully gapped)	$\kappa(T,H)$ (Suetsugu, 2024), Knight shift (Matsumura, 2025)
B_{1u}	Points (k_z)	In/UTe_2 tunneling (Z. Li, 2023) $\kappa(T,H)$ (Hayes, 2024)
B_{2u}	Points (k_y)	Pulse-echo ultrasound (Theuss, 2024) $\kappa(T,H)$ (Hayes, 2024)
B_{3u}	Points (k_x)	Knight shift (Fujibayashi, 2022), Scanning SQUID microscope $\rho_s(T)$ (Iguchi, 2023) Nb/UTe_2 STM (Q. Gu, 2025), QPI (S. Wang, 2025)

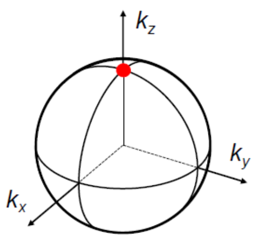

B_{1u}

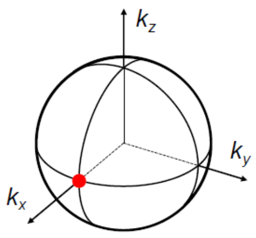

B_{3u}

Superconducting Diamagnetism

Magnetic Fields and Superconductors are not *generally* compatible

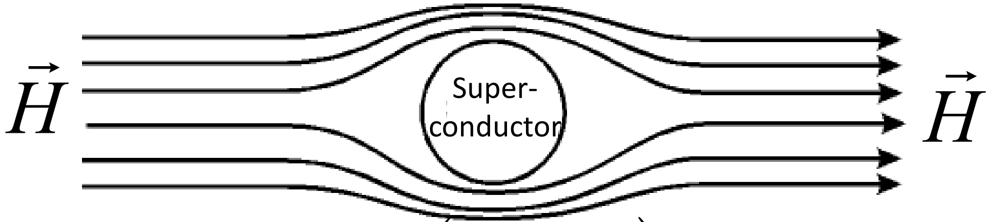

$$\vec{B} = \mu_0\left(\vec{H} + \vec{M}\right) = 0$$

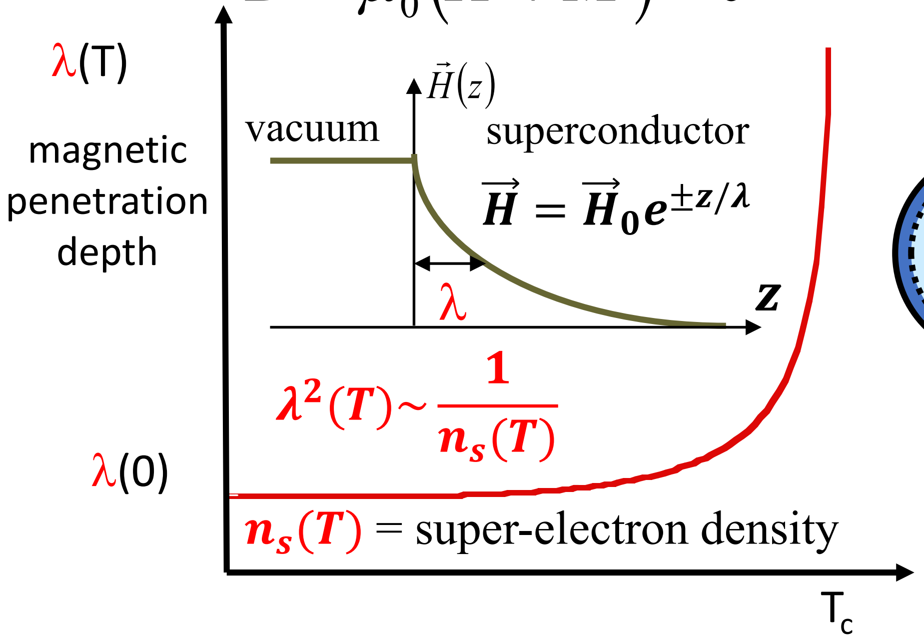

The **Meissner** Effect ($H < H_{c1}$)

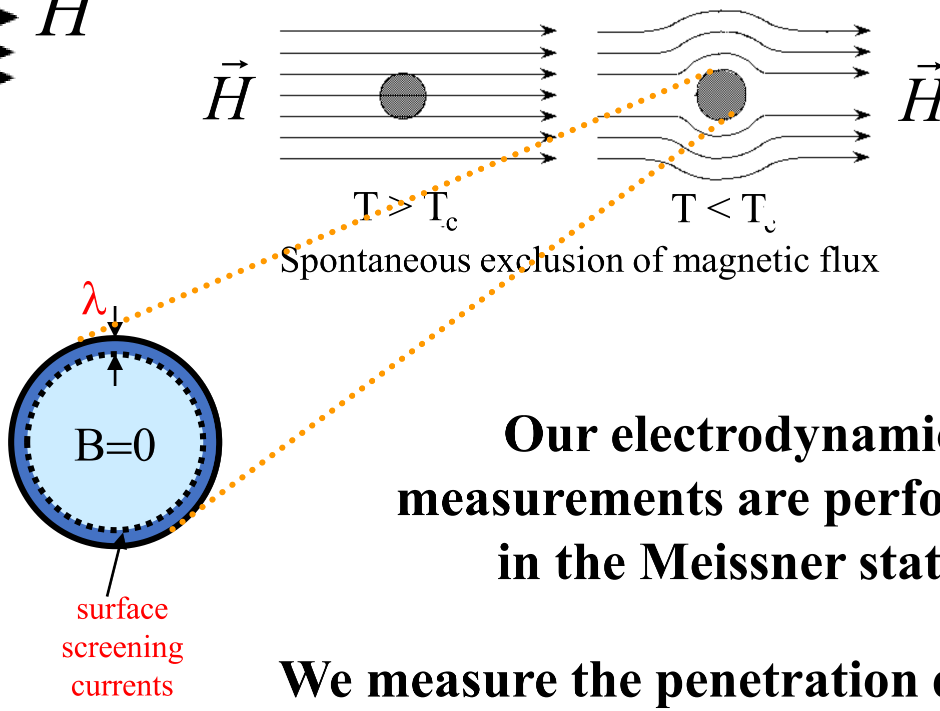

Spontaneous exclusion of magnetic flux

Our electrodynamic measurements are performed in the Meissner state

We measure the penetration depth $\lambda(T)$ and the surface resistance $R_s(T)$

The Low-Energy Electrodynamic Signatures of Nodes

Nodes in the superconducting gap give rise to an abundance of **low-energy excitations** out of the ground state

Nodeless superconductors

$$R_s, \Delta\lambda \propto e^{-\Delta_s(0)/k_B T}$$ for T < $T_c/3$ in a fully-gapped SC

Extrinsic residual losses

$$R_s(T) = R_{BCS}(T) + R_{s,\text{residual}}$$

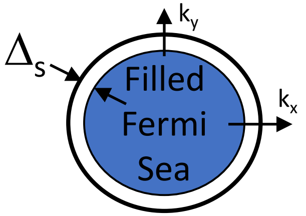

$R_{s,\text{residual}}$ ~ 10^{-9} Ω at 1.5 GHz in Nb SRF accelerator cavities

Line-nodal superconductors

Cuprate (d-wave) SCs have *line nodes* in the energy gap. This leads to power-law behavior of λ(T) and $R_s(T)$ and intrinsic residual losses

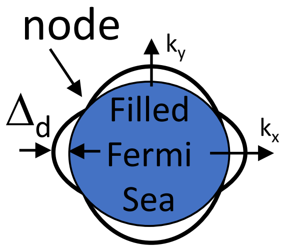

$$\lambda(T) = \lambda(0) + \frac{\ln 2}{\Delta_d} T$$

for $T \ll T_c$

$$R_s = R_{s,Residual} + f(T)$$

$$R_{s,Residual} = \frac{1}{2}\omega^2\mu_0^2\lambda^3\sigma_{00}$$

Intrinsic universal residual conductivity (P. Hirschfeld, 1993):

$$\sigma_{00} = \frac{ne^2\hbar}{m\Delta_d}$$

$R_{s,\text{Residual}}$ ~ 10^{-5} Ω at 10 GHz in $YBa_2Cu_3O_{7-\delta}$

point nodes (single pair)

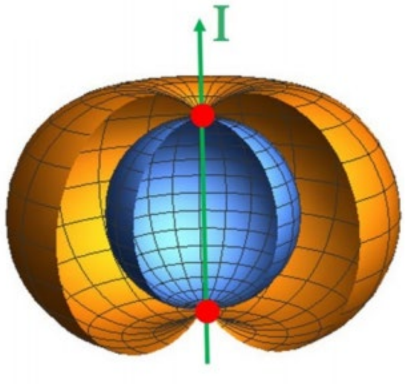

For currents along nodal directions:

$$\lambda_{\parallel}(T) = \lambda_{\parallel}(0) + c\ T^{2}$$

For currents perpendicular to nodal directions:

$$\lambda_{\perp}(T) = \lambda_{\perp}(0) + d\ T^{4}$$

Intrinsic residual conductivity, but no universal value (unless DOS ~ E^2)
(P. Hirschfeld, private communication)

Microwave surface impedance experiment

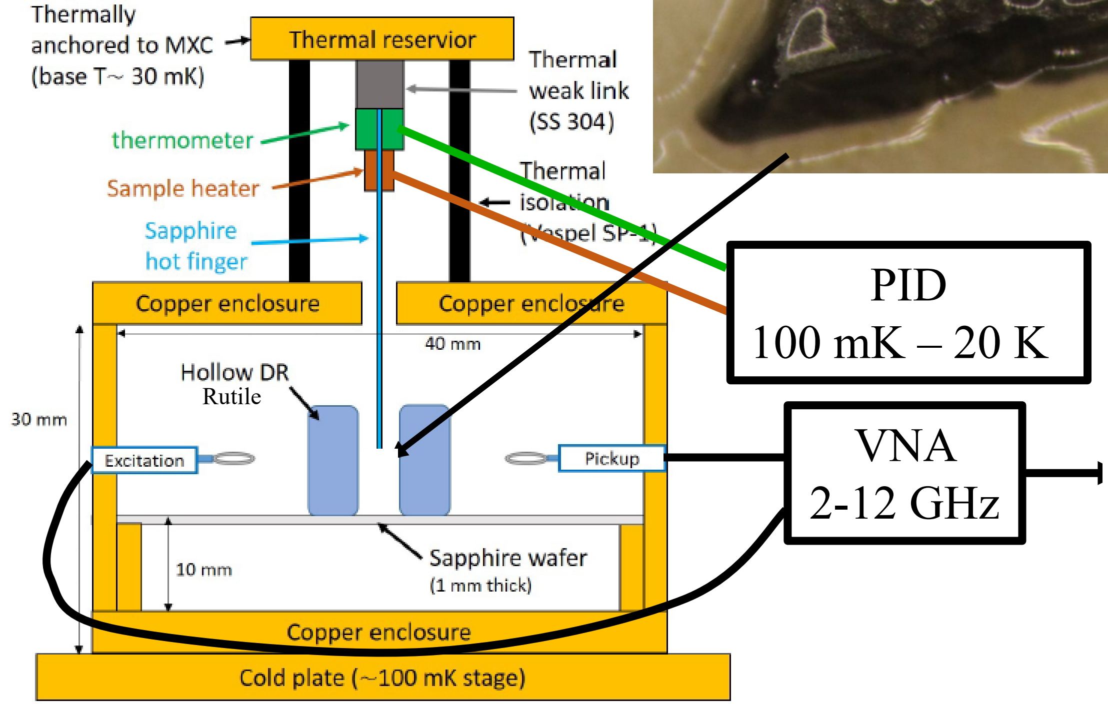

S. Bae, *Nat. Comm.* **12,** 2644 (2021)

1x1 mm

$$R_s = \frac{G}{Q} \qquad \Delta f_0 = f_0(T) - f_0(T_0)$$

$$X_s = -2G\frac{\Delta f_0}{\Delta f_{0,tot}(T_0)} + X_0$$

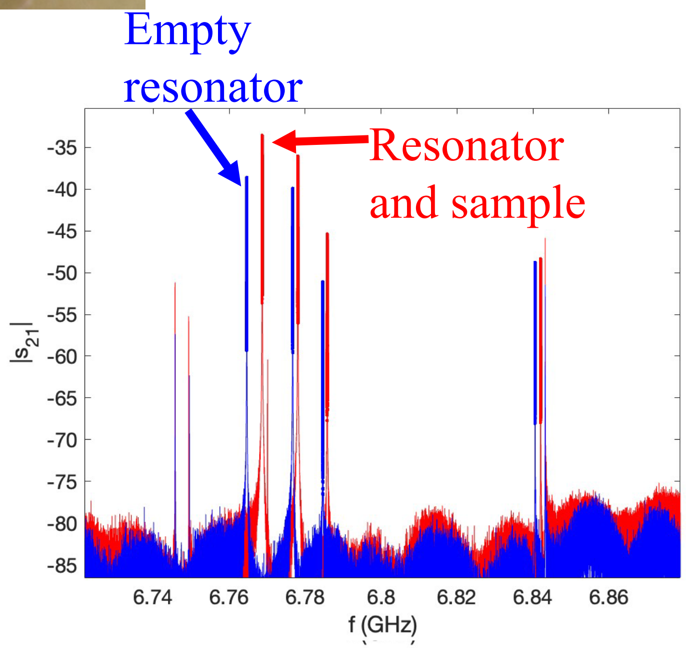

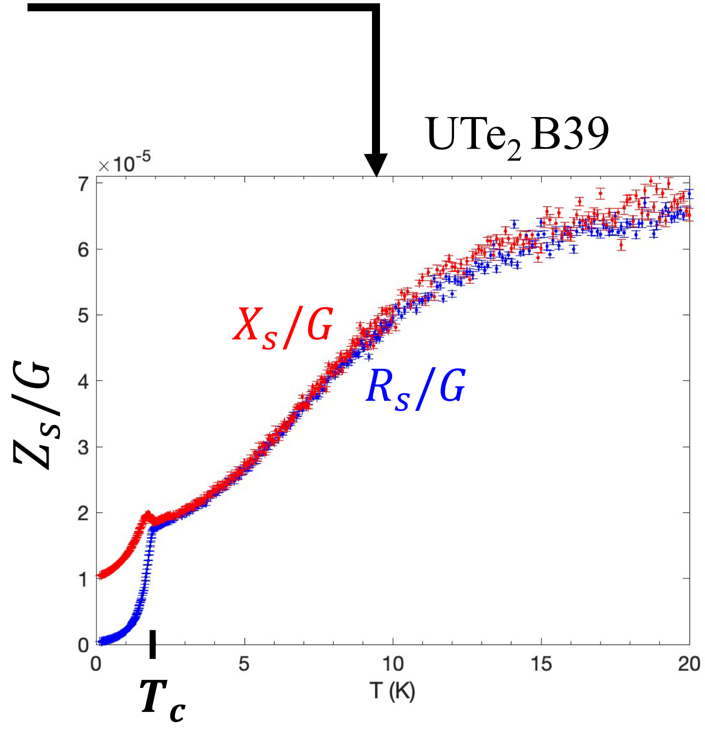

In the **local limit,**

$$Z_s = \sqrt{\frac{i\mu_0\omega}{\sigma}}$$

$$Z_s = R_s + iX_s \longrightarrow \sigma = \sigma_1 - i\sigma_2$$

$$\lambda = 1/\sqrt{\mu_0\omega\sigma_2}$$

Data analysis with *undetermined* G and X_0

- G can be factored out: reveals intrinsic temperature dependence of the data
  ▶ First results for $\boldsymbol{\lambda(T)}$ and $\boldsymbol{R_s(T)}$ at low temperatures
- X_0/G (dimensionless) is strongly constrained by normal-state data

$$\left[\frac{\boldsymbol{Z_s}}{G}\right]\left(T;\frac{X_0}{G}\right)\begin{cases}\left[\frac{R_s}{G}\right](T)=\frac{1}{Q(T)}\\ \left[\frac{X_s}{G}\right]\left(T;\frac{X_0}{G}\right)=\frac{-2\Delta f_0(T)}{f_{0,\mathrm{tot.}}(T_0)}+\frac{X_0}{G}\end{cases}\longrightarrow[\boldsymbol{\sigma}G^2]\left(T;\frac{X_0}{G}\right)=\frac{i\mu_0\omega(T)}{\left[\frac{Z_s}{G}\right]^2\left(T;\frac{X_0}{G}\right)}\longrightarrow\left[\frac{\boldsymbol{\lambda}}{G}\right]\left(T;\frac{X_0}{G}\right)=\frac{1}{\sqrt{\mu_0\omega(T)[\sigma_2G^2]\left(T;\frac{X_0}{G}\right)}}$$

New Approach to Cavity Perturbation Data Analysis

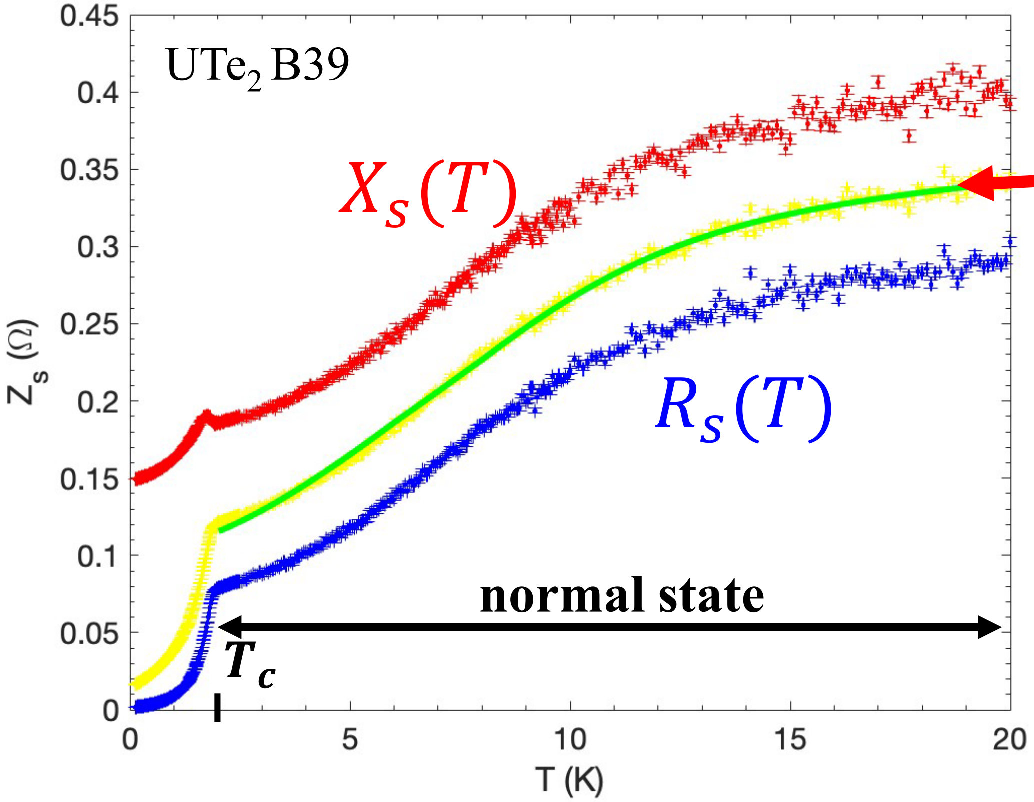

Normal state: Assume Drude model in the local limit:

$$\sqrt{R_s(T)X_s(T)} = w_a R_a(T) + w_b R_b(T) + w_c R_c(T)$$

$$R_i(T) = \sqrt{\mu_0 \omega \rho_i(T)/2}$$

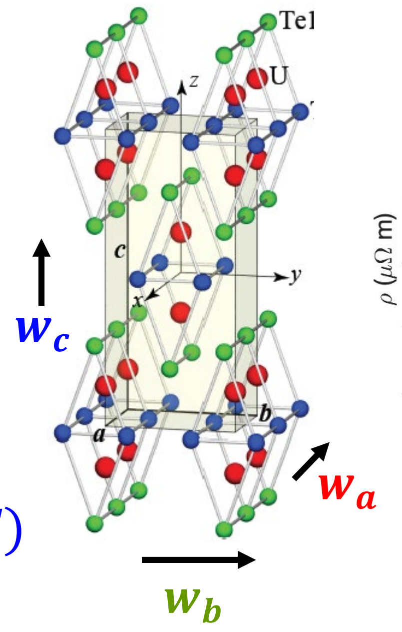

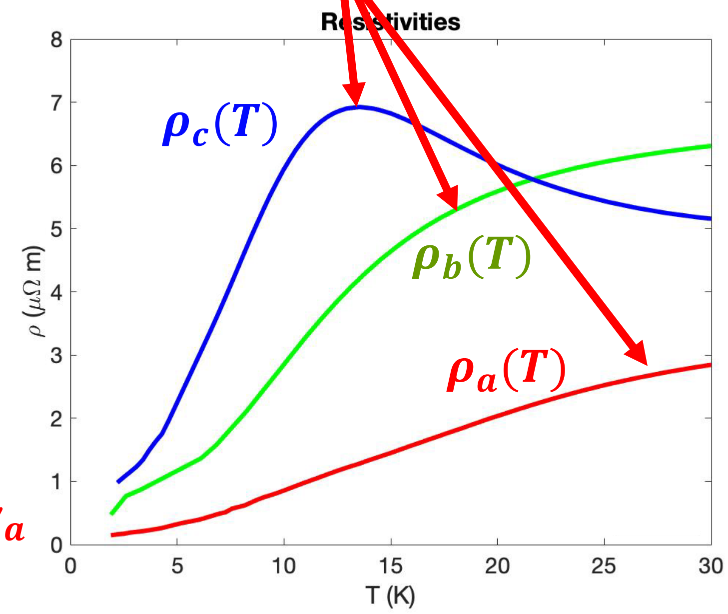

[Y. Eo, *Phys. Rev. B* **106**, L060505]

Full fit gives: (w_a, w_b, w_c, G, X_0) for each mode

This completely determines $R_s(T)$, $\lambda(T)$, $\sigma_1(T)$, $\sigma_2(T)$

- Repeat this for 12-15 modes for each crystal (giving a variety of (w_a, w_b, w_c) weights)

A. Carlton-Jones, *et al.*, PRB 112, 014519 (2025)

Comparison of UTe_2 $\lambda(T)$ with fully-gapped superconductors

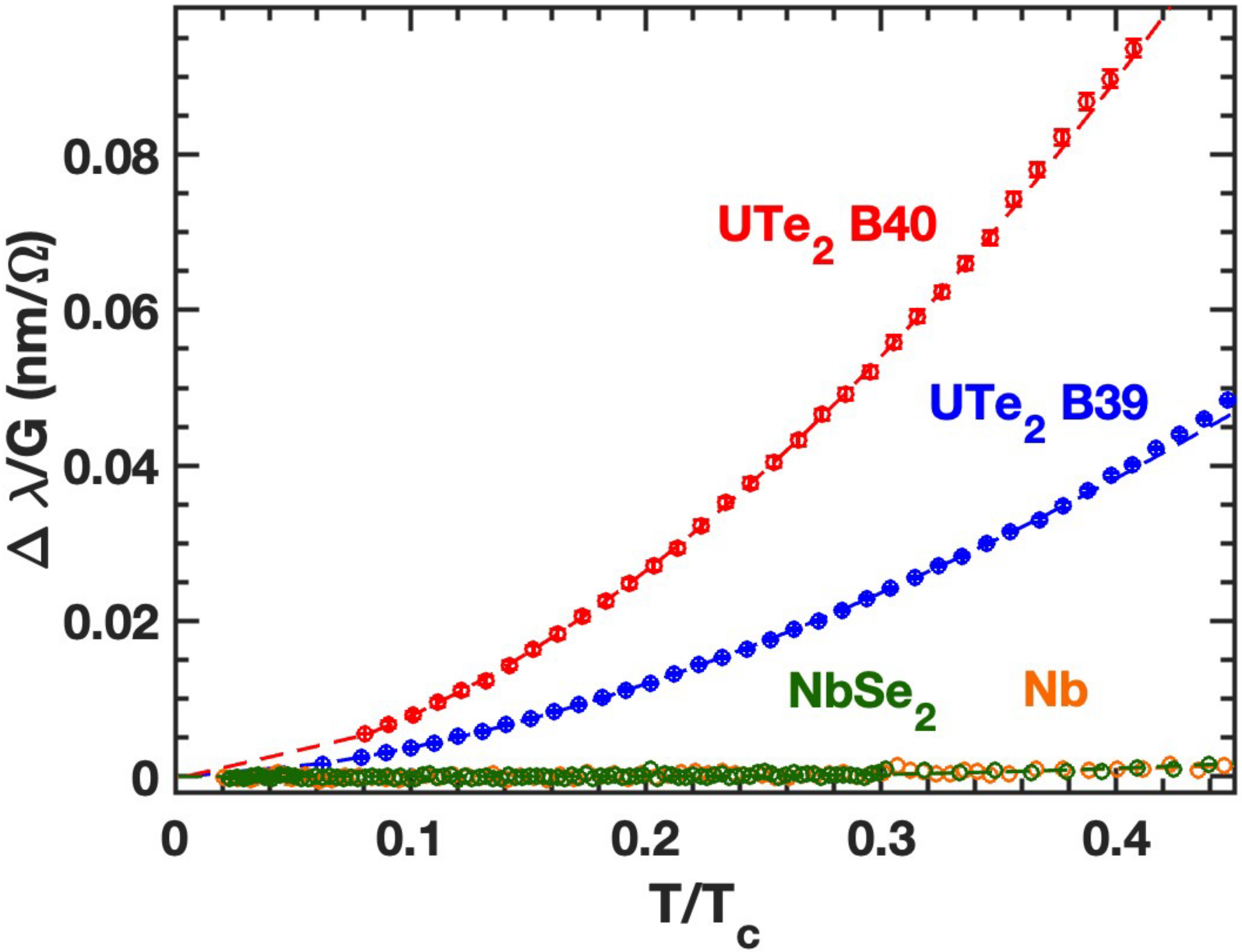

UTe_2: $$\frac{\lambda(T)-\lambda_0}{\lambda_0} = \eta\left(\frac{T}{T_c}\right)^{\alpha}$$

R. A. Klemm, *Z. Phys. B* **72**, 139 (1988)

Nodal superconductivity

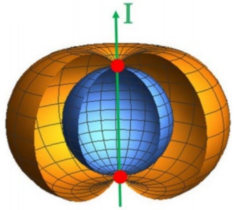

Nb/$NbSe_2$: $$\frac{\lambda(T)-\lambda_0}{\lambda_0} = \sqrt{\frac{\pi\Delta(0)}{2k_BT}}\,e^{-\Delta(0)/k_BT}$$

J. Halbritter, *Z. Phys. A* **243**, 201-219 (1971)

Node-less superconductivity

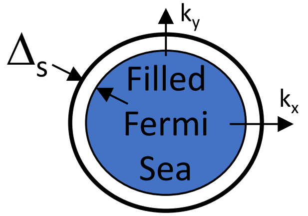

Comparison with nodal theory

(Weak scattering) [R. A. Klemm, *Z. Phys. B* **72**, 139 (1988)]

- Point nodes:
  - || to nodes ($\alpha = 2, \eta = 1.3$)
  - ⊥ to nodes ($\alpha = 4, \eta = 2.1$)
- Line node:
  - || to node ($\alpha = 1$)
  - ⊥ to node ($\alpha = 3$)
- Our data:

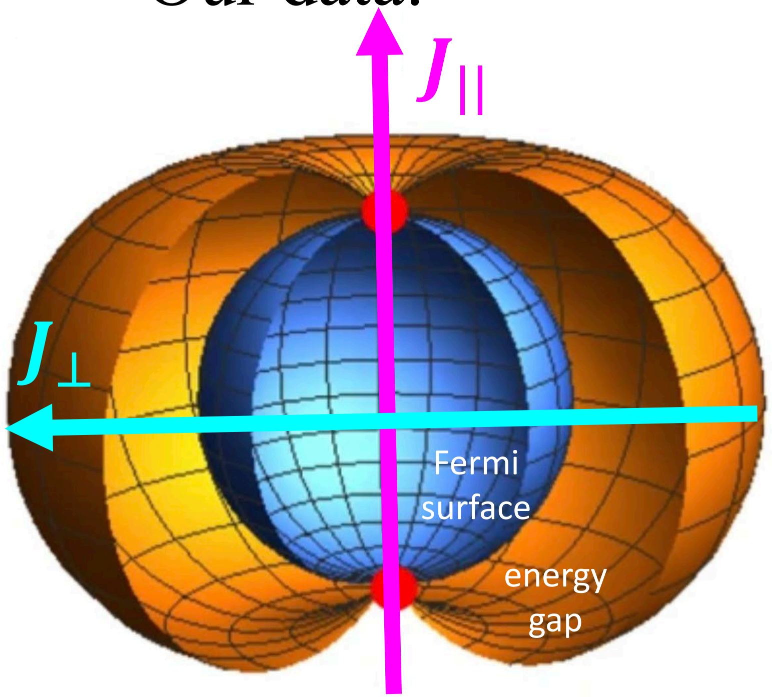

[S. Bae, *Nat. Comm.* **12,** 2644 (2021)]

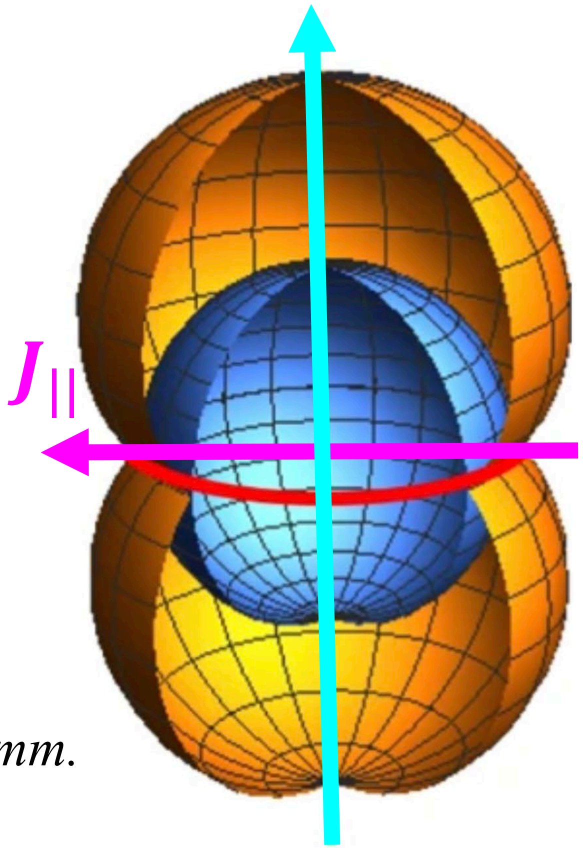

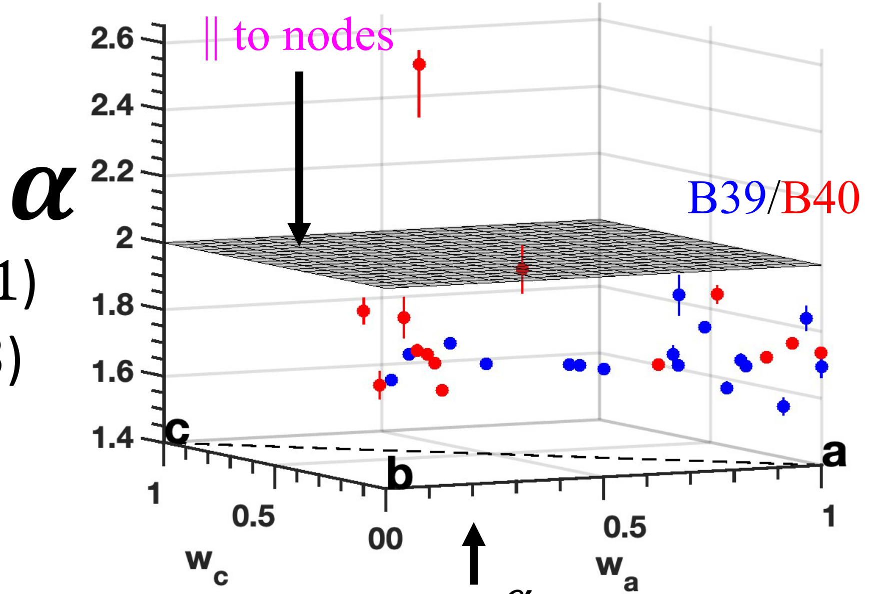

$$\frac{\lambda(T)}{\lambda_0} = 1 + \eta \left(\frac{T}{T_c}\right)^{\alpha}$$

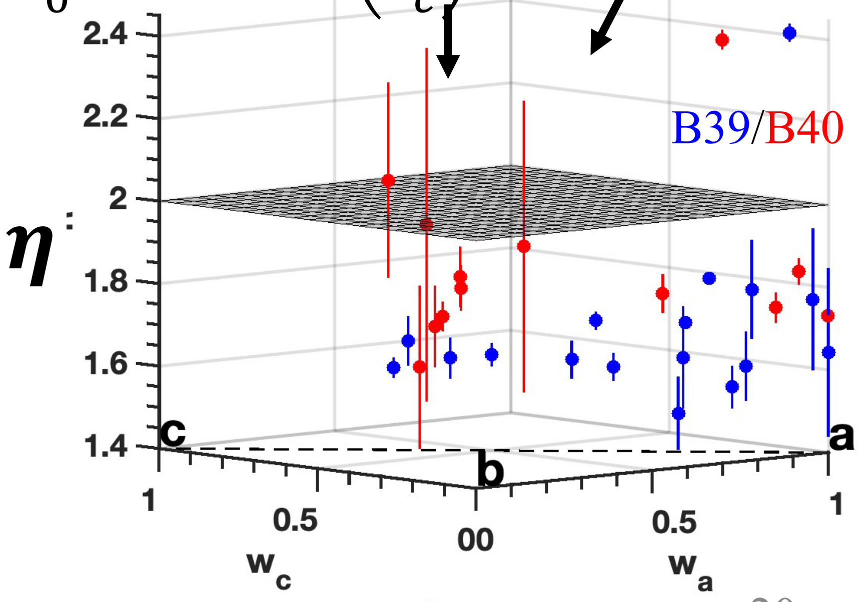

Comparison with nodal theory

(Weak scattering) [R. A. Klemm, *Z. Phys. B* **72**, 139 (1988)]

- Point nodes:
  - || to nodes ($\alpha = 2, \eta = 1.3$)
  - ⊥ to nodes ($\alpha = 4, \eta = 2.1$)
- Line node:
  - || to node ($\alpha = 1$)
  - ⊥ to node ($\alpha = 3$)
- Our data:

Batch	Growth method	T_c (K)	α	η	α_R
B39	CVT2	1.96	1.70 ± 0.08	0.58 ± 0.23	1.70 ± 0.20
B40	CVT2	1.96	1.82 ± 0.25	0.70 ± 0.28	1.86 ± 0.20

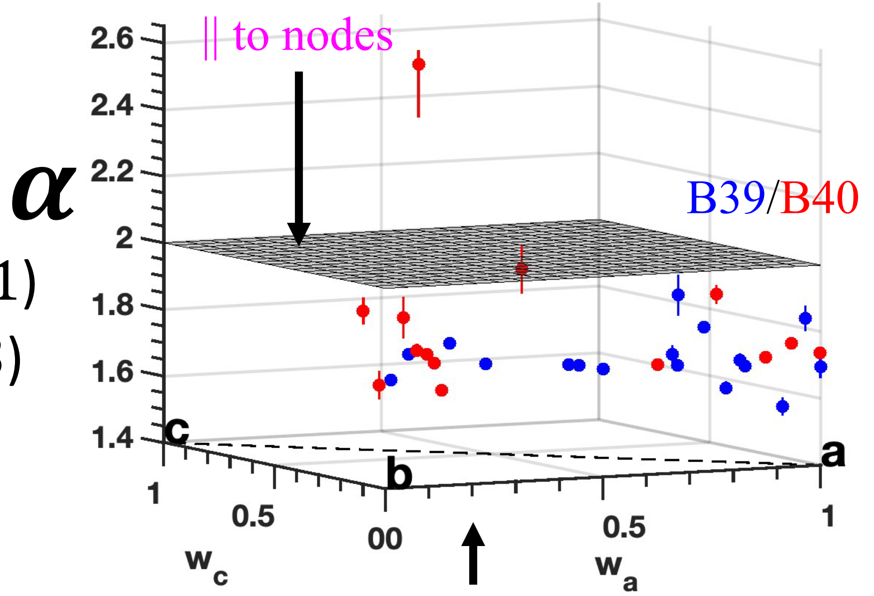

$$\lambda(T)/\lambda_0 = 1 + \eta(T/T_c)^{\alpha}$$

$$R_s(T)/R_0 = 1 + \eta_R(T/T_c)^{\alpha_R}$$

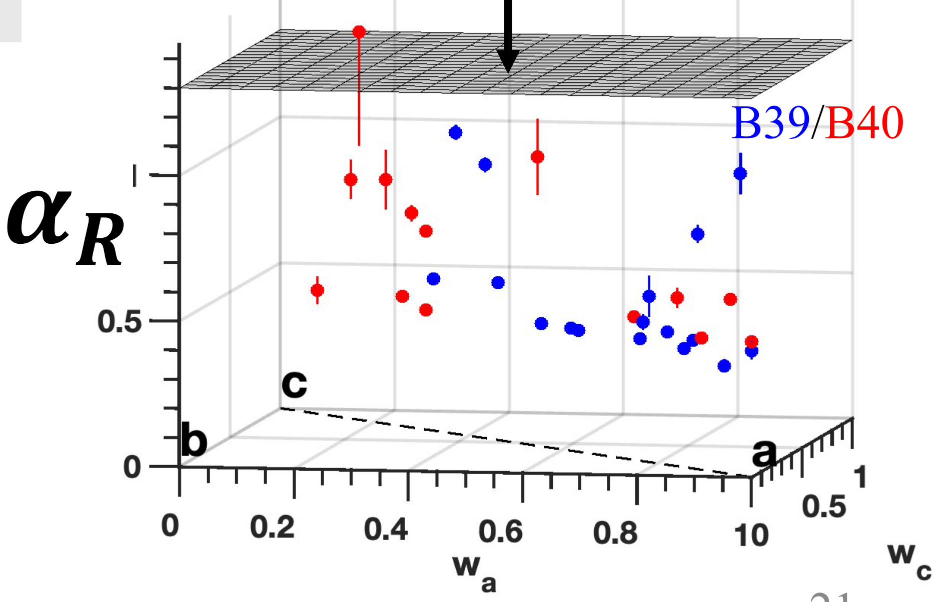

Nodal superconducting gap structure and topological surface states of UTe_2

Hans Christiansen,[1] Max Geier,[2] Brian M. Andersen,[1] and Andreas Kreisel[1]
[1]Niels Bohr Institute, University of Copenhagen, DK-2200 Copenhagen, Denmark
[2]Department of Physics, Massachusetts Institute of Technology, Cambridge, Massachusetts 02139, USA

Phys. Rev. B 112, 054510 (2025)

An abundance of additional nodes, beyond those imposed by symmetry, are required due to the shape of the Fermi surface

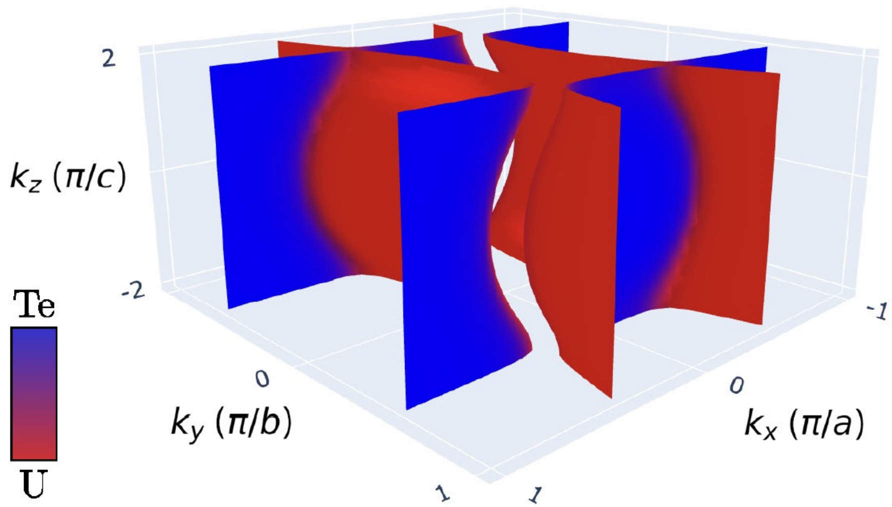

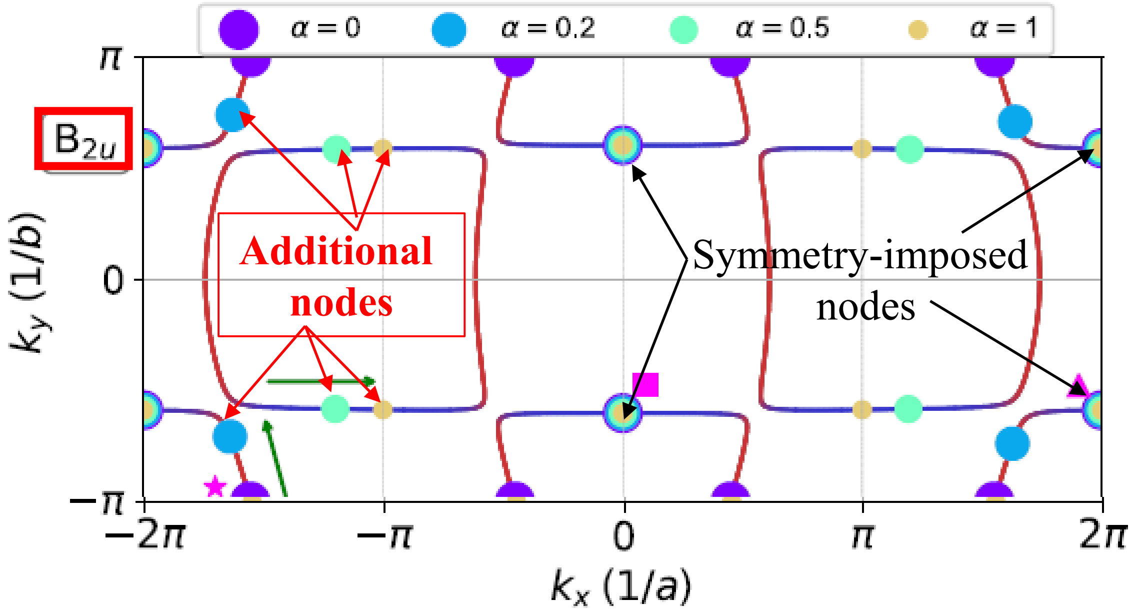

Cut through the Fermi surface at $k_z = 0$

Anisotropy of Residual Losses

~ frequency-independent residual loss

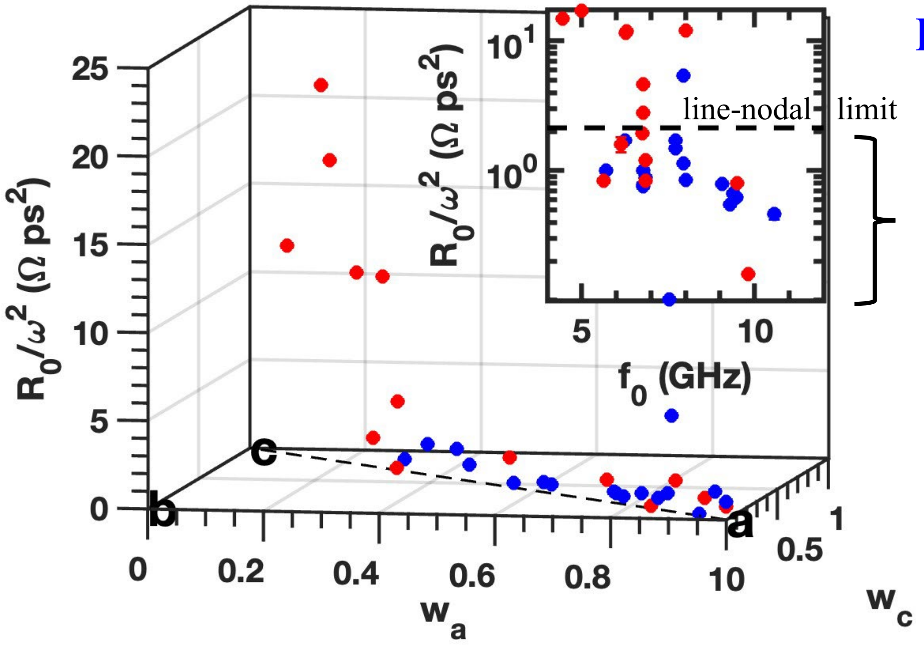

B39/B40

Inconsistent with line-nodal behavior

$$R_0^{\mathrm{line-nodal}} = \mu_0 \omega \lambda_L \frac{\hbar\omega}{2\Delta_{\mathrm{max.}}}$$

[P. J. Hirschfeld, *et al.*, PRL **71**, 3705 (1993)]

[T. C. Wu, *et al.*, PRB **103**, 104517 (2021)]

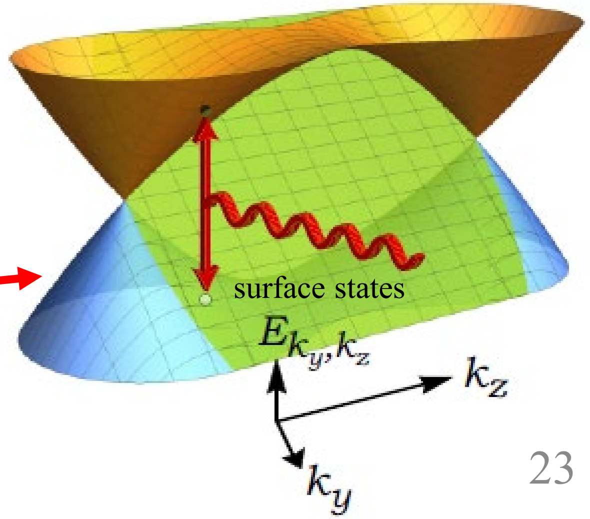

Possible residual loss mechanisms

- [T. C. Wu, *et al.*, PRB **103**, 104517 (2021)] theory:
  - Weyl nodes: $\alpha = 2$ for all directions for Majorana surface states
  - For topological superconductors, larger residual loss is expected along the direction of Weyl nodes
  - Additional loss mechanism associated with transition from surface state to bulk state
- Order parameter collective modes (?)

Anisotropy of Residual Losses

Possible explanations for residual loss anisotropy

- Surface states residing only on particular surfaces
- Nodes in the gap
  - Weyl nodes

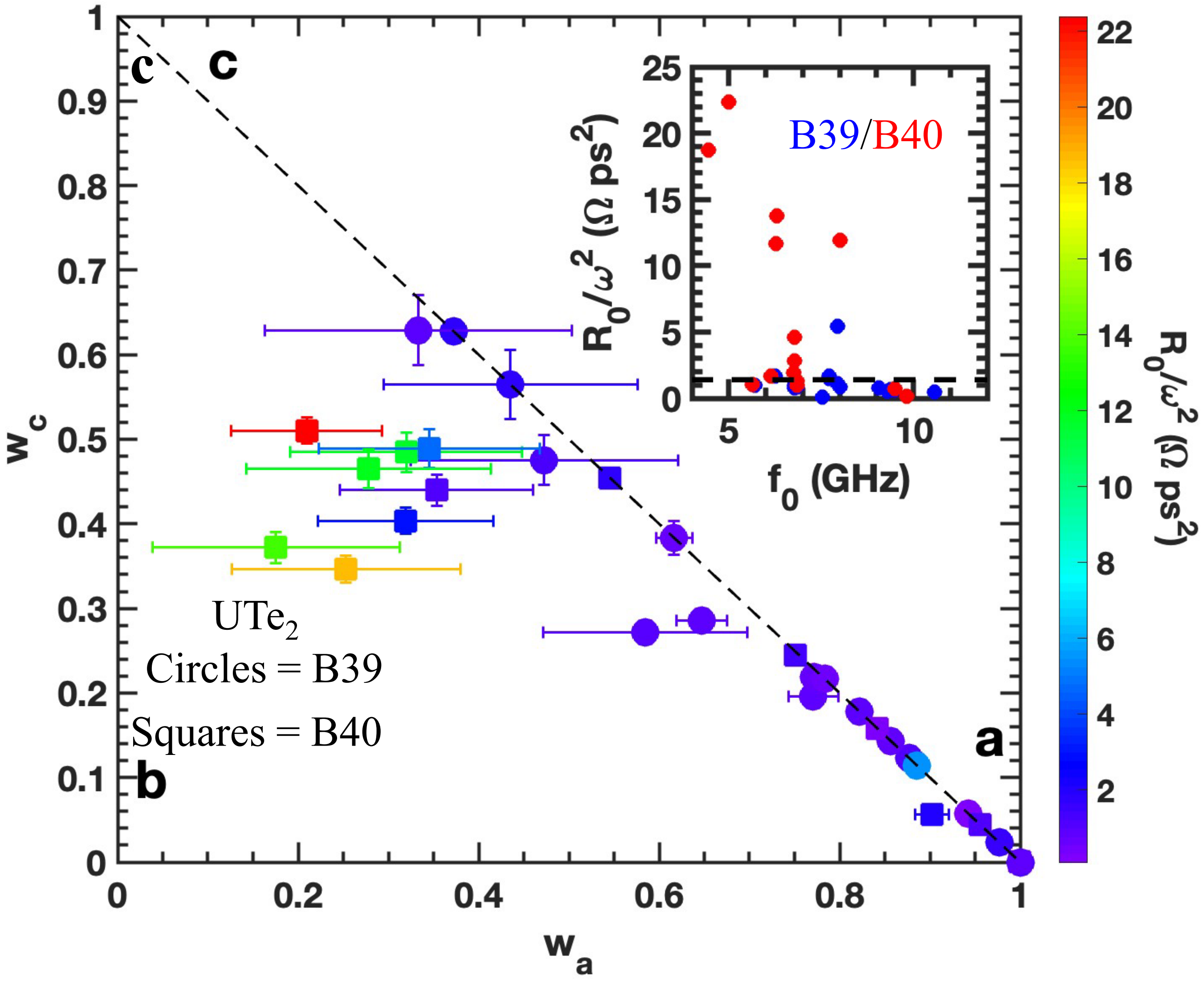

Summary: Properties of UTe_2

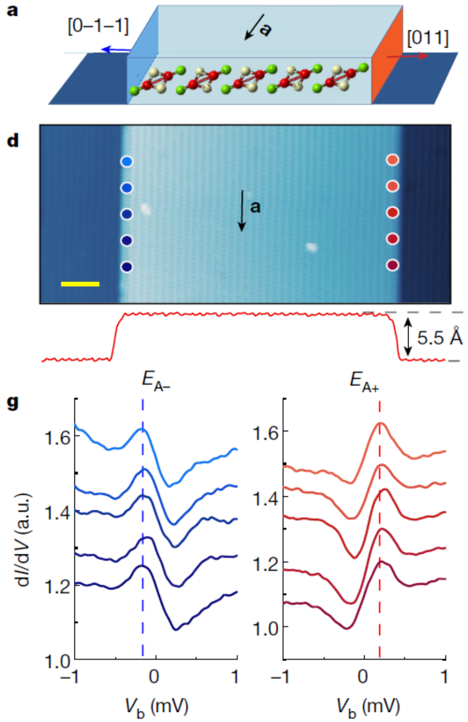

L. Jiao, Nature 579, 523 (2020)

A magnetic-friendly superconductor – probably spin-triplet pairing

A time-reversal preserving superconducting Meissner state

Abundant evidence of point-nodal properties for low-energy excitations

Scanning Tunneling Microscopy shows evidence of

- Chiral in-gap states
- Unusual vortex cores

Hydrostatic pressure dependence shows evidence of competing SC phases

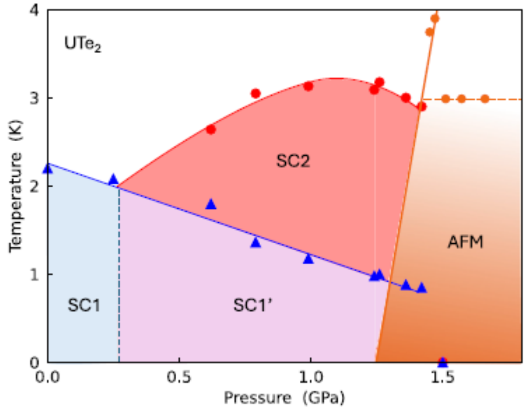

Z. Wu, PRL 134, 236501 (2025)

N. Sharma, ACS Nano 19, 31539 (2025)

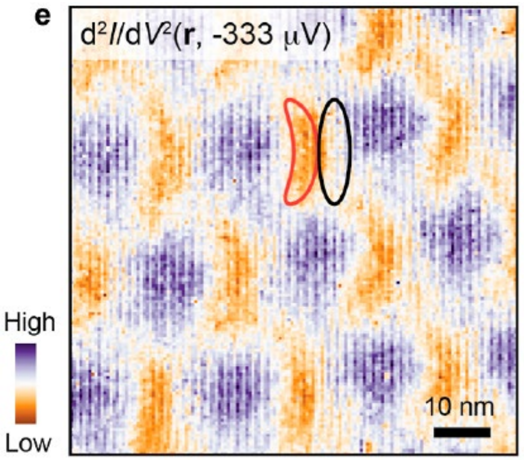

Conclusions

Examined the electrodynamics of several generations of UTe_2 crystals from:

- **5 – 12 GHz**
- **90 mK – 20 K**

Developed a new multi-mode surface impedance data analysis method

Robust $\Delta\lambda \sim T^{\alpha}$ seen in all UTe_2 crystals and modes

- **$\alpha \lesssim 2$ consistent with:**
  - **multiple point-node scenarios,**
  - **Weyl node superconductor**

Substantial residual resistance seen in all UTe_2 crystals and modes

- **Anisotropic**
- **Expected for nodal superconductors**
- **Not consistent with line-nodes**

A. Carlton-Jones, *et al.*, PRB 112, 014519 (2025)

anlage@umd.edu

Work supported by the National Science Foundation through grant # DMR 2004386
and ARO/FSDL under grant W911NF-24-1-0153